ARTICLE NO. 80-4004

680-011

Constrained Optimum Trajectories with Specified Range

0011
0016
0022

Heinz Erzberger* and Homer Lee*
NASA Ames Research Center, Moffett Field, Calif.

The characteristics of optimum fixed-range trajectories whose structure is constrained to climb, steady cruise, and descent segments are derived by application of optimal control theory. The performance function consists of the sum of fuel and time costs, referred to as direct operating cost (DOC). The state variable is range-to-go and the independent variable is energy. In this formulation a cruise segment always occurs at the optimum cruise energy for sufficiently large range. At short ranges (500 n. mi. and less) a cruise segment may also occur below the optimum cruise energy. The existence of such a cruise segment depends primarily on the fuel flow vs thrust characteristics and on thrust constraints. If thrust is a free control variable along with airspeed, it is shown that such cruise segments will not generally occur. If thrust is constrained to some maximum value in climb and to some minimum in descent, such cruise segments generally will occur. The performance difference between free thrust and constrained thrust trajectories has been determined in computer calculations for an example transport aircraft.

Nomenclature

c_f = fuel cost factor, \$/lb (\$/kg)
c_t = time cost factor, \$/hr
D = drag force
D_v, D_{v^2} = first and second partial derivatives of drag with respect to airspeed
d_c = cruise distance
d_f = desired distance to fly
d_{up}, d_{dn} = total climb and descent distances, respectively
E = total aircraft energy in units of altitude
E_c = cruise or maximum energy
E_{copt} = optimum cruise energy
E_i, E_f = initial and final energy
$\dot{E}$ = rate of change of energy
g = acceleration of gravity
H = Hamiltonian, dollars per unit of energy
h = altitude in ft (m)
I_{up}, I_{dn} = components of the Hamiltonian
J = value of performance function in dollars or lbs (kg)
K_{up}, K_{dn} = operands under the minimization operator in H
L = lift force
P = integrand of cost function or cost per unit time
S_{FC} = thrust-specific fuel consumption per hour
$S_{FC(\cdot)^n}$ = nth partial derivatives of S_{FC} with respect to $(\cdot)$
T = thrust, lb (kg)
T_{up}, T_{dn} = climb and descent thrusts, respectively
t = time
t_c = time at end of climb
t_d = time at start of descent
t_f = total mission time
V = true airspeed
V_c = cruise speed
V_{up}, V_{dn} = climb and descent airspeeds
V_w = wind speed along flight path
V_{wup}, V_{wdn} = wind speeds in climb and descent segments, respectively, functions of altitude
W = aircraft weight, lb (kg)
W_f = total mission fuel, lb (kg)
$\dot{W}_f$ = fuel flow rate, lb/h (kg/h)
x = distance flown, n. mi.
x_{up}, x_{dn} = climb and descent distances, running variables
β = parameter defining direction of control perturbations
γ = flight-path angle, rad
ΔR = length of control perturbation
$\Delta T, \Delta V$ = thrust and speed perturbations relative to cruise conditions
$\lambda(E_c)$ = cruise cost at cruise energy E_c, \$/n. mi.
π = throttle setting
π_{up}, π_{dn} = throttle settings in climb and descent, respectively
ψ = costate variable
λ = cruise cost per unit distance
λ_{opt} = optimum cruise cost over all energies, per unit distance

Received Sept. 19, 1978; revision received March 7, 1979. This paper is declared a work of the U.S. Government and therefore is in the public domain. Reprints of this article may be ordered from AIAA Special Publications, 1290 Avenue of the Americas, New York, N.Y. 10019. Order by Article No. at top of page. Member price \$2.00 each; nonmember, \$3.00 each. **Remittance must accompany order.**

Index categories: Flight Operations; Guidance and Control; Navigation, Communciation, and Traffic Control.

*Research Scientist.

Introduction

THE continuing rise in airline operating costs due to higher fuel prices and other factors has stimulated interest in effective methods for trajectory optimization. Recent work has focused on two aspects of this problem: the optimality of steady-state cruise and the simplification of the structure of optimum trajectories. Steady-state cruise is generally not optimum for minimum fuel performance[1]; but the performance penalty of steady-state cruise is unknown, because the actual nonsteady optimum cruise has not been computed. However, if the steady-state cruise satisfies first-order necessary conditions, Speyer[1] shows, in an example, that the performance improvement of a particular (though nonoptimum) cyclic cruise is about 0.1%. This improvement, if representative of the optimum cyclic cruise, is not economically significant. Nevertheless, the determination of the optimum cyclic cruise poses an interesting and unsolved problem.

Even if economically significant, cyclic cruise could not be used in airline operation because it is incompatible with existing air traffic control procedures, disconcerts passengers, and decreases engine life because of increased cycling. Optimum trajectories, to be compatible with typical airline practice, should consist of a climbout, a steady-state cruise, and a descent. Thus, at least for commerical airline applications, the optimum trajectory must be selected from a set of trajectories that is limited a priori to such types.

A formulation of the trajectory optimization problem that constrains the admissible trajectories to those containing

climb, steady cruise, and descent is given in Refs. 2 and 3. In this formulation, energy height was used as the independent or timelike variable in climb and descent, thus forcing energy to change monotonically in these segments. This formulation of the constrained trajectory optimization problem is also adopted in this paper. The use of energy eliminates the integration of a separate adjoint differential equation, thus simplifying the calculus of variations problem.[2,3]

An evaluation of the constrained optimum trajectories by airline operators indicated an interest in the additional constraint of setting the thrust to some maximum during climb and to idle during descent. An examination of this procedure raised the following questions which are investigated in this paper. How do the constraints on thrust and, more generally, the aerodynamic and propulsion characteristics affect the structure of trajectories? Under what condition is the constrained-thrust procedure optimum? What performance penalty is incurred by the constraint on thrust?

Optimal Control Formulation

As stated in the introduction, we assume at the outset that the optimum trajectories have the structure shown in Fig. 1. This structure consists of climb, cruise, and descent segments, with the aircraft energy increasing monotonically in climb and decreasing monotonically in descent. Neglecting flight-path angle dynamics and weight loss due to fuel burn, the point mass equations of motions for flight in the vertical plane are

$$(1/g)\,(\mathrm{d}V/\mathrm{d}t) = [(T-D)/W] - \sin\gamma \tag{1}$$

$$\mathrm{d}h/\mathrm{d}t = V\sin\gamma \tag{2}$$

$$\mathrm{d}x/\mathrm{d}t = V\cos\gamma + V_w \approx V + V_w \tag{3}$$

with the constraint $L = W\cos\gamma$. The along-track wind component V_w may be a function of altitude, but accelerations due to wind shears as well as the vertical wind component can be neglected in this analysis. In airplanes, unlike rockets, the rate of change of weight due to fuel burn introduces negligible dynamic effects in the trajectory optimization. Nevertheless, the effect of weight loss on a trajectory is important but can be accounted for without adding another state variable by treating weight as a slowly changing parameter during trajectory synthesis. If energy is defined as

$$E = h + (1/2g)\,V^2 \tag{4}$$

then the familiar relation for the rate of change of energy is obtained by differentiating Eq. (4) with respect to time and substituting the right-hand sides of Eqs. (1) and (2) in place of $\mathrm{d}V/\mathrm{d}t$ and $\mathrm{d}h/\mathrm{d}t$, respectively:

$$\dot{E} \equiv \mathrm{d}E/\mathrm{d}t = [(T-D)\,V]/W \tag{5}$$

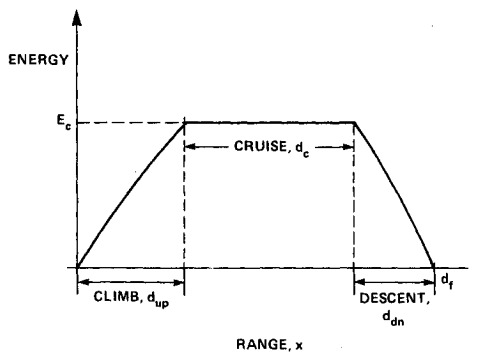

Fig. 1 Assumed structure of optimum trajectories.

The cost function to be minimized is chosen as the direct operating cost of the mission and consists of the sum of the fuel cost and the time cost:

$$J = c_f W_f + c_t t_f \tag{6}$$

where c_f and c_t are the unit costs of fuel and time, respectively. Setting $c_t = 0$ results in the familiar minimum fuel performance function. In integral form, the cost function becomes

$$J = \int_0^{t_f} (\dot{W}_f c_f + c_t)\,\mathrm{d}t \equiv \int_0^{t_f} P\,\mathrm{d}t \tag{7}$$

It is assumed that the time to fly t_f is a free variable, but the distance to fly is a specified quantity d_f. Following the formulation in Ref. 2, we now write the total mission cost as the sum of the costs for the three segments of the assumed trajectory, illustrated in Fig. 1:

$$J = \underbrace{\int_0^{t_c} P\,\mathrm{d}t}_{\text{climb cost}} + \underbrace{(d_f - d_{up} - d_{dn})\lambda}_{\text{cruise cost}} + \underbrace{\int_{t_d}^{t_f} P\,\mathrm{d}t}_{\text{descent cost}} \tag{8}$$

where λ designates the cost of cruising at a given energy E_c. Next, we transform the integral cost terms in Eq. (8) by changing the independent variable from time to energy, using the transformation $\mathrm{d}t = \mathrm{d}E/\dot{E}$:

$$J = \int_{E_i}^{E_c} (P/\dot{E})_{\dot{E}>0}\,\mathrm{d}E + (d_f - d_{up} - d_{dn})\lambda + \int_{E_f}^{E_c} (P/|\dot{E}|)_{\dot{E}<0}\,\mathrm{d}E \tag{9}$$

where E_i and E_f are the given initial climb and final descent energies, respectively. The transformation uses the assumption that the energy changes monotonically in the climb and descent. This places strict inequality constraints on $\dot{E}$, as shown in Eq. (9). Also, in Eq. (9), the integration limits have been reversed in the descent cost term. In this formulation the cost function is of mixed form, containing two integral cost terms and a terminal cost term contributed by the cruise segment.

With the change in independent variable from time to energy, the state equation [Eq. (5)] is eliminated, leaving Eq. (3) as the only state equation. Furthermore, we note that the performance function [Eq. (9)] depends on the distance state x only through the sum of the climb and descent distances $d_{up} + d_{dn}$. Therefore, the state equation for the distance is rewritten in terms of this sum:

$$\mathrm{d}(x_{up} + x_{dn})/\mathrm{d}E = (V_{up} + V_{wup})/\dot{E}]_{\dot{E}>0} + (V_{dn} + V_{wdn})/|\dot{E}|]_{\dot{E}<0} \tag{10}$$

Here the transformation $\mathrm{d}t = \mathrm{d}E/\dot{E}$ was used again. Also, Eq. (10) provides for independence in the choice of climb and descent speeds V_{up} and V_{dn} and the wind velocities V_{wup} and V_{wdn}. Wind velocities in climb and descent are allowed to be independent of each other; generally, different wind conditions will prevail in physically different locations of climb and descent. The wind velocities can also be altitude-dependent. The effect of altitude-dependent winds on the optimum trajectories is discussed in Ref. 3.

Necessary conditions for the minimization of Eq. (9), subject to the state equation [Eq. (10)] are obtained by application of optimum control theory (see, e.g., Ref. 4, p. 71).

Then, the following relations are obtained for the Hamiltonian and costate equations, respectively:

$$H = \min_{\substack{V_{up},V_{dn}\\ \pi_{up},\pi_{dn}}} \left\{ \left(\frac{P}{\dot{E}}\right)_{\dot{E}>0} + \left(\frac{P}{|\dot{E}|}\right)_{\dot{E}<0} + \psi\left[\frac{V_{up}+V_{wup}}{\dot{E}}\right]_{\dot{E}>0} + \frac{V_{dn}+V_{wdn}}{|\dot{E}|}\Big]_{\dot{E}<0} \right\} \tag{11}$$

$$d\psi/dE = -[\partial H/\partial(x_{up}+x_{dn})] = 0 \tag{12}$$

The right-hand side of the Hamiltonian equation is minimized with respect to two pairs of control variables: one pair applicable to climb (V_{up} and π_{up}), the other pair to descent (V_{dn} and π_{dn}). Since each term under the minimization operator in Eq. (11) contains only one of the two pairs of control variables, the minimization simplifies into two independent minimizations: one involving climb controls, the other descent controls. Also, since the right-hand side of the costate equation [Eq. (12)] is zero, ψ is constant.

Transversality Conditions

The transversality conditions are additional necessary conditions that depend on the end-point constraints of state variables.[4] The basic constraint in this problem is that the range of the trajectory be d_f. However, d_f is a parameter in the transformed cost function, Eq. (9), and not a state variable. The final value of the state variable $d_{up}+d_{dn}$ is, in this formulation, subject only to the inequality constraint $d_{up}+d_{dn} \le d_f$. This constraint is, of course, necessary for a physically meaningful result. This inequality constraint can be handled by solving two optimization problems: one completely free ($d_{up}+d_{dn}<d_f$), the other constrained ($d_{up}+d_{dn}=d_f$), and then choosing the trajectory with the lowest cost. Physically, the comparison is between a trajectory wth a cruise segment, and one without a cruise segment. Considering first the free terminal-state case $d_{up}+d_{dn}<d_f$, we obtain the following relation for the final value of the costate ψ:

$$\psi(E_c) = \frac{\partial(d_f - x_{up} - x_{dn})\lambda}{\partial(x_{up}+x_{dn})}\Bigg|_{E=E_c, x_{up}=d_{up}, x_{dn}=d_{dn}} = -\lambda \tag{13}$$

This is the transversality condition for the free final state problem with terminal cost.[4] It shows that the constant costate value is the negative of the cruise cost.

Next, consider the case of no cruise segment. Then, the middle term of Eq. (9) drops out and the performance function contains only the integral cost terms. This is the case of specified final state $d_f = d_{up}+d_{dn}$; the corresponding transversality condition yields $\psi(E_c)=\psi_f$. In practice it is not necessary to compute the constrained terminal-state trajectory if a valid free terminal state trajectory exists, i.e., one for which $d_f > d_{up}+d_{dn}$, since the addition of a terminal constraint can only increase the cost of the trajectory. Therefore, this case is not considered further in this paper.

In both cases the choice of costate determines a particular range. Since the functional relationship between these variables cannot be determined in closed form it is necessary to iterate on the costate value in order to achieve a specified range d_f.

The last necessary condition applicable to this formulation is obtained by making use of the fact that the final value of the timelike independent variable E is free. Its final value is the upper limit of integration E_c in Eq. (9). Application of results in Ref. 4 provides the following condition:

$$(H + \{\partial[(d_f - d_{up} - d_{dn})\lambda(E)]/\partial E\})_{E=E_c} = 0 \tag{14}$$

which, when evaluated and simplified, becomes

$$\{H + [d_c(d\lambda/dE)]\}_{E=E_c} = 0 \tag{15}$$

where d_c is the cruise distance.

Condition (15) has the following physical interpretation. The value of the Hamiltonian H evaluated at cruise energy E_c is [after substituting Eq. (13) into Eq. (11)] the minimum increment in the sum of climb cost and descent cost to make a unit increment in cruise energy. The product $d_c(d\lambda/dE)_{E=E_c}$ is the increment in cruise cost resulting from a unit change in cruise energy. Condition (15) requires the optimum trajectory to be such that the sum of these two increments be zero for a given cruise distance d_c and cruise energy E_c.

Dependence of Optimum Trajectories on Range

Equation (15), together with knowledge of the salient characteristics of the cruise cost λ and the Hamiltonian H, can be used to determine the structural dependence of the optimum trajectories on range.

Cruise cost at a cruise energy E_c and cruise speed V_c is computed from the relation

$$\lambda(E_c,V_c) = [P(T,E_c,V_c)]/(V_c+V_w) \quad \text{constraints: } \begin{Bmatrix} T=D \\ L=W \end{Bmatrix} \tag{16}$$

where the denominator is the ground speed in the flight-path direction. Examination of the term containing λ in the relation for the performance function (9) shows that the value for λ should be as small as possible at each cruise energy in order to minimize the total cost J. Therefore, the cruise speed dependence of λ is eliminated by minimizing the right side of Eq. (16) with respect to V_c:

$$\lambda(E_c) = \min_{V_c} P(T,E_c,V_c)/(V_c+V_w) \tag{17}$$

In this paper, λ and V_c are always assumed to be the optimum cruise cost and cruise speed, respectively, at a particular cruise energy E_c.

Except in high wind shear, the cruise cost as a function of cruise energy exhibits the roughly parabolic shape shown in Fig. 2. For subsonic transport aircraft, the minimum of the cruise cost with respect to energy occurs close to the maximum energy boundary. This characteristic of the cruise cost prevails for essentially all values of the performance function parameters c_f and c_t. The quantities defining the optimum cruise conditions are E_{copt} and λ_{opt}. In Eq. (15), the derivative of the cruise cost function multiplies the cruise distance. Except under extreme wind shear conditions, the derivative is monotonic and crosses the zero axis at $E_c = E_{copt}$.

By distributing the minimization operator in Eq. (11) and substituting Eq. (13) in Eq. (11), H can be decomposed into

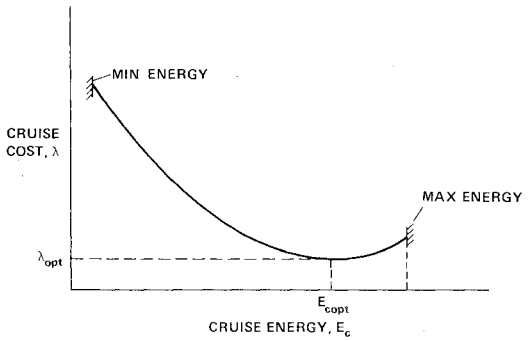

Fig. 2 Cruise cost function.

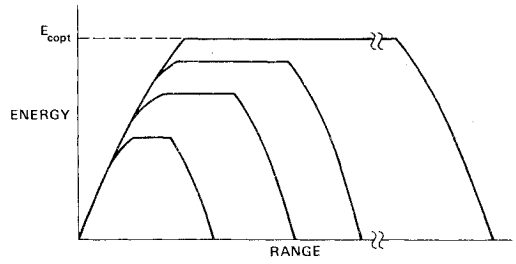

Fig. 3 Energy vs range, $H>0$ at E_c.

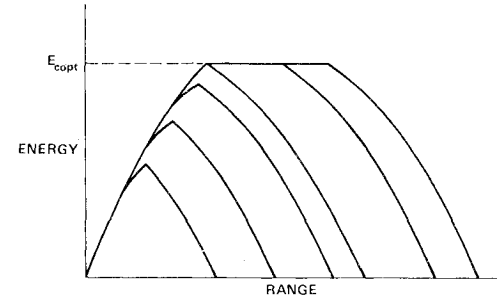

Fig. 4 Energy vs range, $H=0$ at E_c.

climb and descent components as follows:

$$H[E,\lambda(E_c)] = I_{up} + I_{dn} \tag{18}$$

where

$$I_{up} = \min_{\substack{V_{up} \\ \pi_{up}}} \left[\frac{P - \lambda(V_{up} + V_{wup})}{\dot{E}} \right]_{\dot{E}>0}$$

$$I_{dn} = \min_{\substack{V_{dn} \\ \pi_{dn}}} \left[\frac{P - \lambda(V_{dn} + V_{wdn})}{|\dot{E}|} \right]_{\dot{E}<0} \tag{19}$$

In the preceding section, the Hamiltonian, evaluated at $E=E_c$, was interpreted as the cost penalty to achieve a unit increase in cruise energy. Extensive numerical studies of Eq. (18) for several comprehensive models of subsonic turbofan aircraft show $H[E_c,\lambda(E_c)] \geq 0$, for $E_c \leq E_{copt}$. Moreover, the minimum cost penalty for increasing energy I_{up} is always positive and that for decreasing energy I_{dn} is negative; but the sum has never been found negative for models of currently used turbofans. While these characteristics have been established for several aircraft models, they are not intended to imply a generalization to all aircraft, since no physical laws prevent H from being negative.

Consider first the case where $H[E_c,\lambda(E_c)]>0$. Then, Eq. (15) can be solved for the cruise distance d_c:

$$d_c = -H[E_c,\lambda(E_c)]/(d\lambda/dE)_{E=E_c} \tag{20}$$

Since $d\lambda/dE<0$, but approaches zero as E_c approaches E_{copt}, the cruise distance must increase without limit as E_c approaches E_{copt}. Our numerical studies have shown that the value of H tends to decrease as E_c increases, but not enough to change this trend. Figure 3 shows the resulting family of trajectories, assuming $H>0$ for all values of E_c. In this case, interestingly, nonzero cruise segments occur at short ranges and at energies below the optimum cruise energy E_{copt}. Optimum cruise is approached asymptotically at long range.

Consider next the case where $H[E_c,\lambda(E_c)]=0$. Then $d_c=0$, i.e., no cruise segment is present for $d\lambda/dE<0$. However, Eq. (15) shows that d_c can be nonzero if $d\lambda/dE=0$. This implies that for $H=0$, cruise flight is optimum only at the optimum cruise energy E_{copt}. Figure 4 shows the family of trajectories for this case.

Thrust Optimization for Minimum Fuel Trajectories

Evaluation of the Hamiltonian equation would be simplified if one of the pairs of control variables, airspeed or thrust, could somehow be eliminated a priori from the minimization. Since the pair of throttle settings, π_{up} and π_{dn}, is thought to be near its limit, we shall look for conditions where extreme settings of the throttle are optimum. The remainder of the paper examines only the minimum fuel case $c_f=1$ and $c_t=0$, with winds set to zero in order to simplify the derivation. However, the results can be extended to the more general cost function.

For minimum fuel performance, the two terms in the Hamiltonian equation, Eq. (19), become

$$I_{up} = \min_{\pi_{up}, V_{up}} K_{up} \qquad I_{dn} = \min_{\pi_{dn}, V_{dn}} K_{dn} \tag{21a}$$

where

$$K_{up} \equiv \left[\frac{\dot{W}_f - \lambda V_{up}}{(T-D)\,V_{up}/W} \right]_{T(\pi_{up})>D}$$

$$K_{dn} \equiv \left[\frac{\dot{W}_f - \lambda V_{dn}}{|T-D|\,V_{dn}/W} \right]_{T(\pi_{dn})<D} \tag{21b}$$

An accurate model for thrust and fuel flow generally includes the functional dependencies, $T(\pi,V,h)$ and $\dot{W}_f(\pi,V,h)$. In addition, these functions must be corrected for nonstandard temperatures and bleed losses.

In some previous work on aircraft trajectory optimization,[5] a simpler model for fuel flow and thrust was used:

$$\dot{W}_f = TS_{FC}(V,h) \qquad T_{min}(V,h) \leq T \leq T_{max}(V,h) \tag{22}$$

The critical assumption in Eq. (22) is independence of the specific fuel consumption S_{FC} from thrust. The virtue of this model lies in the insight it yields into the minimum fuel problem. If Eq. (22) is substituted into Eqs. (21b), one obtains

$$K_{up} = \frac{S_{FC}W}{V_{up}} \left[\frac{T_{up} - (\lambda/S_{FC})\,V_{up}}{T_{up} - D} \right]_{T_{up}>D}$$

$$K_{dn} = \frac{S_{FC}W}{V_{dn}} \left[\frac{T_{dn} - (\lambda/S_{FC})\,V_{dn}}{|T_{dn} - D|} \right]_{T_{dn}<D} \tag{23}$$

For any fixed values of V_{up} or V_{dn}, the operand functions for the minimization of K_{up} and K_{dn} are hyperbolas with poles at $T=D$. The numerator zero must be to the left of the pole on the thrust axis for energies less than cruise energy. Figure 5 is a typical plot of these functions. Clearly, maximum thrust minimizes K_{up} and idle thrust minimizes K_{dn} for any $E<E_c$, proving that the limiting values of thrust are optimum for this propulsion model throughout the climb and descent trajectories. This result also implies that the departure from the extreme thrust values found for the more general propulsion model is directly attributable to the nonlinear dependence of fuel flow on thrust. Conversely, the need for throttle setting optimization can be determined a priori from the fuel flow vs thrust dependence for a particular engine. Such data are found in the engine manufacturer's performance handbook.

Evaluation of Hamiltonian at Cruise

We have seen in a preceding section that the value of the Hamiltonian computed at cruise energy E_c determines the structure of the trajectories near cruise. Here we shall relate the existence of cruise below E_{copt} to specific engine and

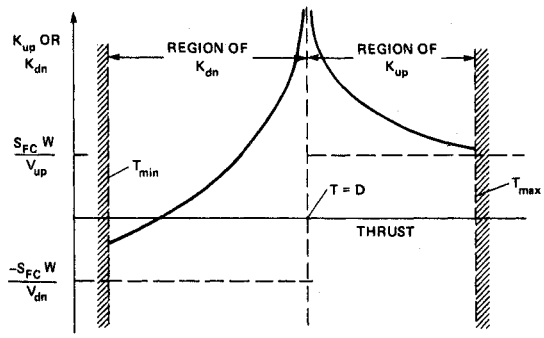

Fig. 5 Illustrating dependence of K_{up} and K_{dn} on thrust.

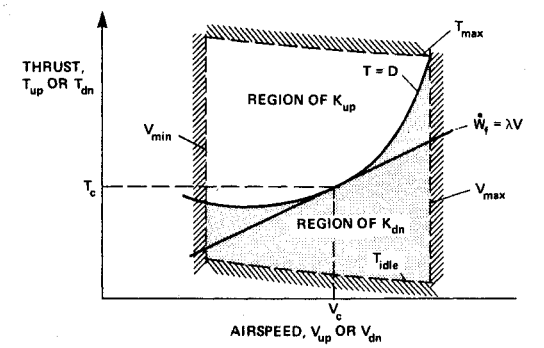

Fig. 6 Loci of $T=D$ and $\dot{W}_f=\lambda V$ in control space at $E=E_c$.

aerodynamic model parameters. This is done by substituting truncated Taylor series expansions of fuel flow and drag as functions of airspeed and thrust into the expression for the Hamiltonian. The location of the minimum with respect to the controls as well as the value of H can then be determined as functions of the Taylor series coefficients at $E=E_c$.

How should one pick the point in the control space about which to make the expansion? Computational experience in Refs. 2 and 3 has shown that the minimum is in the neighborhood of the optimum cruise speed and throttle setting, corresponding to the given cruise energy. This suggests that the cruise controls should be picked for the expansion point.

The fuel flow and drag functions expanded to second order about the cruise controls $T=T_c$, $V=V_c$ are

$$\dot{W}_f = T_c S_{FC} + (T_c S_{FC_T} + S_{FC})\Delta T + T_c S_{FC_V}\Delta V + \tfrac{1}{2}(2S_{FC_T} + T_c S_{FC_{T^2}})\Delta T^2 + (T_c S_{FC_{TV}} + S_{FC_V})\Delta V\Delta T + \tfrac{1}{2}T_c S_{FC_{V^2}}\Delta V^2 + \text{higher-order terms} \tag{24}$$

$$D = D(V_c,E_c) + D_v\Delta V + \tfrac{1}{2}D_{v^2}\Delta V^2 + \text{higher-order terms} \tag{25}$$

The subscripts to S_{FC} and D designate the partial derivatives with respect to the subscripted variable. Note that the expansion allows for a general fuel flow model in which specific fuel consumption can be thrust-dependent.

Before substituting Eqs. (24) and (25) into the expression for H, we observe that H is singular at cruise with $T=T_c$ and $V=V_c$, because both numerator and denominator are identically zero at that point. Figure 6 plots the loci of the numerator and denominator zeros of K_{up} and K_{dn} in the control space at $E=E_c$. It is proved in the Appendix that the locus of numerator zeros is tangent to the locus of denominator zeros at the optimum cruise controls. For $E<E_c$ the two loci have no points in common. The two loci can be tangent but cannot cross, since otherwise controls would exist that would make the Hamiltonian infinitely negative, a result ruled out as physically meaningless.

Upon substituting Eqs. (24) and (25) into Eqs. (21) using the tangency condition (A4) derived in the Appendix, the following expressions for K_{up} and K_{dn} at cruise energy are obtained:

$$\left.\begin{matrix} K_{up} \\ \text{or} \\ K_{dn} \end{matrix}\right\} = \frac{W}{(V_c+\Delta V)} \frac{A}{|\Delta T - D_v\Delta V - \tfrac{1}{2}D_{v^2}\Delta V^2|} \tag{26}$$

where

$$A = (T_c S_{FC_T} + S_{FC})\Delta T - (D_v S_{FC} + T_c S_{FC_T} D_v)\Delta V + \tfrac{1}{2}(2S_{FC_T} + T_c S_{FC_{T^2}})\Delta T^2 + (T_c S_{FC_{TV}} + S_{FC_V})\Delta V\Delta T + \tfrac{1}{2}T_c S_{FC_{V^2}}\Delta V^2$$

Terms above second order have been neglected since we are investigating a small neighborhood of the cruise point. Expression (26) represents K_{up} if the quantity under the absolute value sign is positive and K_{dn} if it is negative.

Since the cruise point at $\Delta T=0$ and $\Delta V=0$ gives the undefined value of 0/0 for Eq. (26), it is necessary to evaluate the limit as ΔT and ΔV approach zero. If the limit exists, it must be independent of the direction from which the cruise point is approached. To compute the limit and investigate the neighborhood of the cruise point, a polar coordinate system centered at the cruise point is used to define control perturbations. Let ΔR and β define control perturbations ΔT and ΔV as follows:

$$\Delta T = (D_v+\beta)\Delta V \tag{27}$$

$$\Delta V = \Delta R/\sqrt{1+(\beta+D_v)^2}$$

$$\Delta T = \Delta R(\beta+D_v)/\sqrt{1+(\beta+D_v)^2} \tag{28}$$

The parameter β defines a direction relative to the reference direction of the line $\Delta T=D_v\Delta V$. The reference direction $\beta=0$ is excluded from the control space since it is along the direction of the locus of $T=D$ at the cruise point.

After substituting Eqs. (28) into Eq. (26) and taking the limit of the resulting expressions as $\Delta R\to 0$, one obtains for any $\beta\neq 0$

$$K_{up}]_{lim} = (W/V_c)(S_{FC}+T_c S_{FC_T})$$
$$K_{dn}]_{lim} = (-W/V_c)(S_{FC}+T_c S_{FC_T}) \tag{29}$$

The limit is thus well defined, since it is independent of the approach direction in each region. However, it remains to be shown that the limit value is in fact the minimum of Eq. (26) with respect to the perturbation controls. This question is investigated for two cases: one where S_{FC} is independent, the other where it is dependent on thrust.

Case A: S_{FC} Independent of Thrust

Along the direction defined by $\Delta V=0$, i.e., along the thrust direction, Eq. (23) can be used directly to determine the dependence of the functions on T_{up} and T_{dn} under the minimization operator. Since at $V=V_c$, $D(V_c,E_c) = T_c = (\lambda/S_{FC})V_c$, Eq. (23) reduces to

$$K_{up} = (W/V_c)S_{FC} \qquad K_{dn} = (-W/V_c)S_{FC} \tag{30}$$

showing that at the cruise speed V_c these functions are independent of thrust. This result is not restricted to small perturbations relative to the cruise thrust. Along other directions, the truncated Taylor series form [Eq. (26)] must be used. After setting to zero all thrust-dependent derivatives

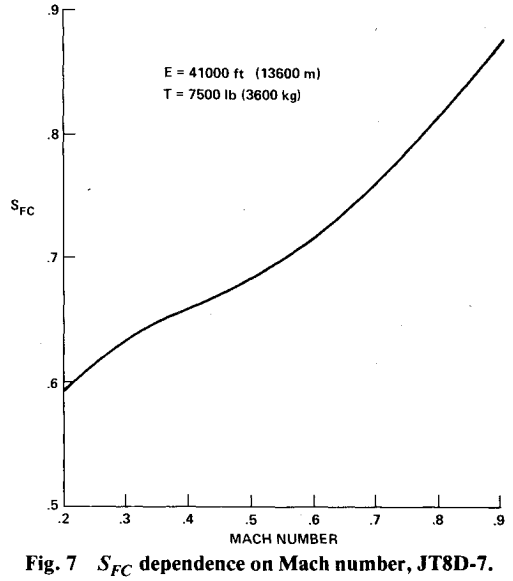

Fig. 7 S_{FC} dependence on Mach number, JT8D-7.

and substituting Eqs. (28) into Eq. (26), the following expression is obtained:

$$\left.\begin{matrix} K_{up} \\ \text{or} \\ K_{dn} \end{matrix}\right\} = \frac{WS_{FC}}{(V_c + \Delta V)} \times \left[\frac{\pm 1 + \dfrac{(2S_{FC_V}(|\beta| + D_v) + T_c S_{FC_{V^2}})\Delta R}{2|\beta| S_{FC}\sqrt{1+(\beta+D_v)^2}}}{\left| 1 - \dfrac{D_v^2 \Delta R}{2|\beta|\sqrt{1+(\beta+D_v)^2}} \right|} \right] \quad (31)$$

where the positive sign applies to K_{up} and the negative sign to K_{dn}. The characteristics of these functions depend on the drag and specific fuel consumption derivatives. The drag derivatives D_v and D_v^2 are both positive, since the aircraft will certainly operate on the "front" side of the thrust-required curve. The dependence of S_{FC} on speed at cruise energies for a typical turbofan engine currently in service exhibits a slight upward curvature above Mach 0.4, as shown in Fig. 7, implying that both S_{FC_V} and $S_{FC_{V^2}}$ are positive in the range of interest between Mach 0.4 and 0.9. The slight curvature of S_{FC} indicates that a quadratic function can accurately model the Mach number dependence of S_{FC} in the Mach range of interest and not just in a small neighborhood of the expansion point. Also, at typical cruise conditions one finds that $D_v^2 > (2S_{FC_V} D_v + T_c S_{FC_{V^2}})$. Therefore, for any β, the denominator of Eq. (31) goes to zero before the numerator does as ΔR is increased from an initial value of zero. Moreover, the slope of the operand function with respect to ΔR increases as β approaches zero. The effect of ΔV can be neglected, since $V_c \gg \Delta V$.

These observations lead to the conclusion that the functions in Eq. (31) slope upward in all directions as ΔR increases, except in the direction parallel to the thrust axis, along which the slope is level. Figure 8 shows a family of plots of the operand functions as β varies over its range. The limiting values of these functions at the cruise point $(\pm W/V_c) S_{FC}$ are therefore also the global minimums, and the value of the Hamiltonian, which is the sum of the two components, is zero. At the cruise energy, furthermore, the optimum climb and descent speeds are equal to the optimum cruise speed. The optimum climb and descent thrusts at that point are arbitrary since the Hamiltonian is independent of them.

By applying these results to Eq. (20), it now follows that the structure of the optimum trajectories near cruise is given by the family of trajectories in Fig. 4. Specifically, no cruise segment occurs except at optimum cruise energy E_{copt}.

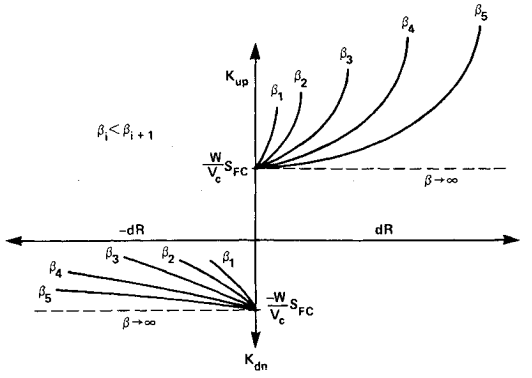

Fig. 8 Dependence of operand function on dR and β at cruise energy E_c.

By combining results from this and the preceding section, the important result follows that, for the assumed engine model, the optimum trajectories, the corresponding optimum controls, and the performance are not affected by constraining the thrust to extreme values in the climb and descent segments.

Case B: S_{FC} Thrust Dependent

A complete investigation of the neighborhood of the cruise point analogous to Case A requires estimates of the various thrust-dependent derivatives in Eq. (26). However, understanding of this case can be obtained by examining the functions in Eq. (26) only along the thrust direction, i.e. for $\Delta V = 0$. Under that assumption, Eq. (26) simplifies to the following expression:

$$\left.\begin{matrix} K_{up} \\ \text{or} \\ K_{dn} \end{matrix}\right\} = \frac{WS_{FC}}{V_c}\left[\pm 1 + \frac{T_c S_{FC_T}}{S_{FC}} + \frac{|\Delta T|}{2S_{FC}}\left(2S_{FC_T} + T_c S_{FC_{T^2}}\right)\right] \quad (32)$$

where the plus sign and $\Delta T > 0$ are chosen for K_{up} and the negative sign and $\Delta T < 0$ for K_{dn}.

This simplified approach focuses attention on the derivatives S_{FC_T} and $S_{FC_{T^2}}$, which are crucial for this case. The characteristics of these derivatives can be deduced from plots of S_{FC} vs thrust, in Fig. 9. These plots, and those in Fig. 7, were derived from the operating instructions manual of a typical inservice turbofan.[6] Obviously, the assumption of a thrust-independent S_{FC} is grossly violated for this engine, since at low thrust values the S_{FC} curves approach infinity; that is, they become undefined. However, at typical climb or cruise thrusts, corresponding to the upper half of the thrust range, the variation in S_{FC} is only about 5%.

Fuel flow is also plotted in Fig. 9. The dashed line through the origin gives the best constant S_{FC} approximation to the fuel flow function. Comparison indicates an excellent match at high thrust, but an error of as much as 1200 lb/h (550 kg/h) at low thrust. For some applications the assumption of a constant S_{FC} could be adequate if fuel flow errors at very low or idle thrust settings can be tolerated.

For the upper two-thirds of the thrust range, quadratic functions provide good fits to the S_{FC} curves. Therefore, one can use the second-order Taylor-series expansion at the cruise point to estimate S_{FC} for fairly large deviations of thrust from cruise thrust.

The thrust in climb or cruise is typically larger than the thrust at which S_{FC} is a minimum in Fig. 9. Both S_{FC_T} and $S_{FC_{T^2}}$ will, therefore, be greater than zero, and so will the coefficient of ΔT in Eq. (32). It follows that the slope of Eq. (32) as a function of ΔT is greater than zero for K_{up} and less than zero for K_{dn}. In other words, along the thrust direction these functions have a strong minimum at the cruise point, whereas in case A they were level along this direction. Along

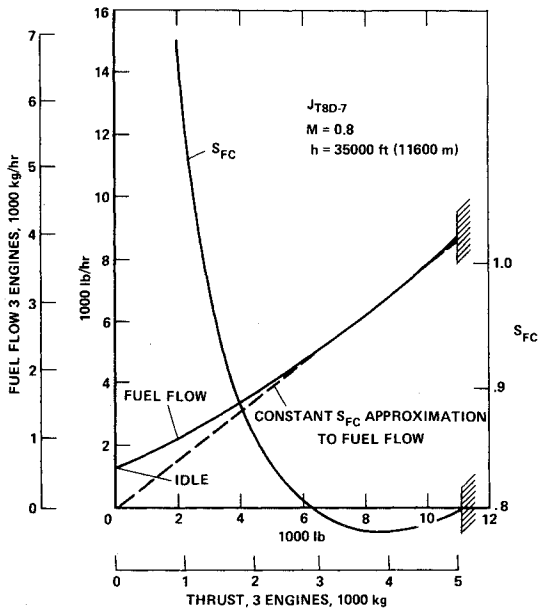

Fig. 9 S_{FC} and fuel flow vs thrust, typical cruise conditions.

other directions, the investigation of case A has shown a positive slope. Thus, if thrust is an unconstrained control variable along with airspeed, so that the cruise point lies in the interior of the control region, then the optimum climb and descent thrusts and airspeeds will converge toward the optimum cruise thrust and airspeed as the climb and descent energies approach the cruise energy. It should be noted that this holds for all cruise energies, including those less than the optimum cruise energy, E_{copt}. Since the Hamiltonian is again zero at the cruise energy, it follows that the structure of the optimum trajectories as a function of range is identical to that of case A and is illustrated by Fig. 4. Computer calculations for this case in Ref. 2, using a similar engine model, showed that the thrust is either maximum or idle for about three-fourths of the energy range between initial and cruise energies and then departs from the extremum values so as to converge smoothly to the value at cruise as cruise energy is approached.

Consider now the case where thrust is constrained to some maximum in climb and is idle in descent. In that case, the minimum at the cruise point is not accessible since it does not lie in the region of permissible controls. Also, unlike case A, the thrust dependence of K_{up} and K_{dn} in Eq. (32) does not disappear along the thrust direction at $V = V_c$. Therefore, it is unlikely that at the minimum the sum of the two terms will be zero. The Hamiltonian is, in fact, greater than zero at any cruise energy. In order to show this, note in Fig. 9 that as thrust decreases, S_{FC} increases without bound. It follows that I_{dn} will be less negative than it would be if S_{FC} were thrust-independent and therefore will be insufficient to cancel I_{up} at cruise energy, resulting in a positive value for the Hamiltonian. This was shown earlier to give rise to nonzero cruise segments below the optimum cruise energy. Thus, the structure of the optimum trajectories for the constrained thrust case is given by the family of trajectories in Fig. 3.

Some Numerical Results

Calculations of various types of optimum trajectories (minimum fuel and cost) have been carried out for the Boeing 727-100 and the McDonnell Douglas DC-10 aircraft using a digital computer implementation of the algorithm described in this paper. The models used in this program contain typical propulsion and aerodynamic data, including thrust-dependent specific fuel consumption and separate idle thrust and fuel flow models. The program also compensates for weight loss due to fuel burn as well as allowing the user to choose between the constrained and unconstrained thrust cases. The program is designed to augment or be a substitute for the computerized flight planning systems now used by airlines. A complete discussion of the results obtained in these calculations is beyond the scope of this paper. As an example of the results, Table 1 gives summary data for two minimum fuel and two minimum DOC trajectories for the 727-100.

For the case of minimum fuel performance, the difference in fuel consumption between the constrained and free thrust optimum trajectories is 63 lb (29 kg), or about 1%. For the case of minimum DOC performance, the difference is \$0.03/n. mi., or again about 1%. In both cases the differences have been found consistently, though dependent on range and aircraft weight. These differences, while not large, are about at the threshold (1% level) where they are considered significant in airline operating economics.

For both performance functions, the optimum cruise distances for the constrained thrust cases are a small percentage (11% and 18%) of the total range. These results indicate that, for this engine, the specific fuel consumption dependence on thrust does not have a strong influence on the trajectories. The DOC penalty of flying minimum fuel trajectories is seen to be \$0.14/n. mi., or 6%, while the fuel penalty for flying minimum DOC trajectories is about 300 lb (136 kg), or 7%. Each airline must evaluate the signficance of the fuel and DOC differences between the trajectories in light of its schedules and route structures.

Table 1 Optimum trajectories for 200 n. mi. range Boeing 727-100 with JT8D-7 engines—1965 United States standard atmosphere[a]

Cost function	Thrust constraint	Cruise or maximum altitude, ft	Cruise distance, n. mi.	Fuel, lb (kg)	Time, min:\$	DOC,[b] \$/n. mi.
Minimum fuel	Climb power in ascent, idle in descent	29,500	34	4570 (2072)	37:11	2.54
	No constraints except operating limits	31,000	0	4507 (2044)	36:40	2.51
Minimum DOC[b]	Climb power in ascent, idle in descent	30,400	22	4909 (2226)	30:01	2.40
	No constraints except operating limits	30,500	0	4812 (2183)	29:47	2.37

[a] Initial weight = 136,000 lb (61,750 kg); initial and final altitudes = sea level each; initial and final airspeeds = 210 knots each.
[b] Based on c_f = \$0.056/lb of fuel and c_t = \$410/h.

The fuel cost and time cost factors used in these calculations are estimates from a United States airline in mid-1977. These factors vary with time and between airlines.

A comparison can also be made between the performance of optimum and currently used procedures. Such a comparison for a model of the DC-10 flying a 220 n. mi. range yielded a 7% fuel savings for the minimum fuel trajectories.[7]

Conclusions

The approach to trajectory optimization presented here has led to a rather detailed understanding of the characteristics of the optimum trajectories. The approach also lends itself to a numerically stable computer implementation that can be incorporated in an airline flight planning system or, ideally, in an onboard performance management system. Furthermore, trajectories generated by this method can serve as benchmarks for evaluating other (suboptimum) algorithms. This possibility is especially intriguing at this time in view of the strong current effort in industry to develop the so-called onboard optimum performance computers.

Two pairs of opposing assumptions, constrained vs free thrust and dependence vs independence of specific fuel consumption on thrust, played pivotal roles in determining the characteristics of the optimum trajectories. If the assumption of specific fuel consumption independent of thrust is justified, constrained thrust trajectories are identical to free thrust trajectories in structure and performance for the minimum fuel case. However, when the realistic dependence of specific fuel consumption on thrust is taken into account, there will be a difference in both performance and structure between constrained and free thrust cases. The actual numerical differences in performance depend on the propulsion and aerodynamic models as well as other factors and must be determined by computer calculations.

Appendix

It is to be proved that the loci of $\dot{W}_f - \lambda V = 0$ and $T - D = 0$ are tangent at the cruise point, assuming that the cruise point at $T = T_c$, $V = V_c$ is a minimum of the cruise cost $\dot{W}_f / V$ along the locus $T - D = 0$. This is equivalent to proving that the cruise point lies on both loci and that the slopes of the loci are identical at that point.

That the cruise point satisfies $\dot{W}_f - \lambda V = 0$ follows from the sequence of relations below:

$$(\dot{W}_f - \lambda V)\Big]_{\substack{T=T_c \\ V=V_c}} = V\left(\frac{\dot{W}_f}{V} - \lambda\right)\Big]_{\substack{T=T_c \\ V=V_c}}$$

$$= V_c\left\{\left(\frac{\dot{W}_f}{V}\right)\Big]_{\substack{T=T_c \\ V=V_c}} - \lambda\right\} = V_c(\lambda - \lambda) = 0$$

To prove that the slopes are identical, compute the gradient of $\dot{W}_f - \lambda V$:

$$\nabla(\dot{W}_f - \lambda V)$$

$$= i\left[TS_{FC_V} - (TS_{FC}/V)\right]_{\substack{T=T_c \\ V=V_c}} + j\left[TS_{FC_T} + S_{FC}\right]_{\substack{T=T_c \\ V=V_c}} \quad \text{(A1)}$$

The perpendicular unit vectors i and j point in the speed and thrust directions, respectively. Now write λ as a function of the perturbation ΔV:

$$\lambda = [(T_c + D_v \Delta V) S_{FC}(T_c + D_v \Delta V, V_c + \Delta V)] / (V_c + \Delta V) \quad \text{(A2)}$$

Since, by assumption, λ has a minimum at $V = V_c$, set the derivative of λ with respect to ΔV equal to zero. This yields the following relation:

$$\lambda = D_v S_{FC} + T_c\left(S_{FC_T} D_v + S_{FC_V}\right) = T_c S_{FC}/V_c \quad \text{(A3)}$$

Next, compute the gradient of $(T-D)(V/W)$ at the cruise point:

$$\nabla(T-D)(V/W)\Big]_{\substack{T=T_c \\ V=V_c}} = (V_c/W)[i(-D_v) + j] \quad \text{(A4)}$$

The slope of Eq. (A1) relative to the i direction is given by

$$\text{Slope} = \frac{T_c S_{FC_T} + S_{FC}}{T_c S_{FC_V} - (T_c S_{FC}/V_c)} \quad \text{(A5)}$$

After substituting Eq. (A3) in place of $T_c S_{FC}/V_c$ in Eq. (A5), the slope simplifies to $-1D_v$, which is identical to the slope of Eq. (A4).

References

[1] Speyer, J.L., "Nonoptimality of the Steady-State Cruise for Aircraft," *AIAA Journal*, Vol. 14, Nov. 1976, pp. 1604-1610.

[2] Erzberger, H., McLean, J.D., and Barman, J.F., "Fixed-Range Optimum Trajectories for Short Haul Aircraft," NASA TN D8115, Dec. 1975.

[3] Barman, J.F. and Erzberger, H., "Fixed-Range Optimum Trajectories for Short-Haul Aircraft," *Journal of Aircraft*, Vol. 13, Oct. 1976, pp. 748-754.

[4] Bryson, A.E., Jr. and Ho., Y-C., *Applied Optimal Control*, Blaisdell, Waltham, Mass., 1969, Chap. 2.

[5] Schultz, R.L. and Zagalsky, N.R., "Aircraft Performance Optimization," *Journal of Aircraft*, Vol. 9, Feb. 1972, pp. 108-114.

[6] Specific Operating Instructions, JT8D-7 Commercial Turbofan Engines, Pratt and Whitney Aircraft, E. Hartford, Conn., Jan. 1969.

[7] Bochem, J.H., Mossman, D.C., and Larrier, P.D., "Simulator Evaluation of Optimal Thrust Management/Fuel Conservation Strategies for Airbus Aircraft on Short Haul Routes," Final Report, NASA Contractor Report NAS 2-9174, Ames Research Center, Jan. 1977.